Environmental Science and Pollution Research (2021) 28:41794–41806
https://doi.org/10.1007/s11356-021-13677-0

RESEARCH ARTICLE

A new technique of seawater intrusion control: development of geochemical cutoff wall

Ezzeddine Laabidi[1] · Rachida Bouhlila[1]

Received: 20 October 2020 / Accepted: 24 March 2021 / Published online: 31 March 2021

Abstract

The construction of a subsurface dam and/or physical cutoff barriers is one of the most known techniques used to prevent seawater intrusion during excessive exploitation of freshwater from a coastal aquifer. This method is widely used in many sites around the world (Japan, Brazil, India, Burkina Faso…). In this study, we present an innovative technique for constructing subsurface barriers based on geochemical reactions. A calcite cutoff wall is developed by mixing two aqueous solutions Na_2CO_3 and $CaCl_2$ under pCO_2 equal to $3.16{\cdot}10^{-4}$ bar. The deposition of calcite in the mixing zone induces a high clogging, which greatly reduces the porosity and then the permeability of the aquifer into the injection zone. We use GEODENS code to study the effect of a developed geochemical cutoff wall on saltwater intrusion and to assess their protective effect on preventing seawater intrusion. The GEODENS code can solve these equations by a finite element procedure; it can handle density-dependent flow, transport, and geochemical reactions in porous media. The effect of depth and location of the geochemical cutoff wall is tested and results showed a significant reduction of seawater intrusion penetration length. According to the budget used in many barrier construction projects, we have shown that the developed geochemical cutoff wall presented in this work could produce a lower seawater intrusion penetration length than the traditionally used barriers at a very lower cost.

Keywords Geochemical cutoff wall · Coastal aquifer management · Seawater intrusion control · Clogging · Calcite precipitation · Porosity change

Introduction

The greatest challenge that faces hydrogeologists today is water security. Increased population, extensive land use, and socio-economic activities induce an overexploitation of groundwater resources and various contamination of stored water resources especially in coastal zones where population and activities are concentrated. Numerous technologies have been developed to counteract the leaks into groundwater or the protection of these resources against various pollutant solutions that can invade the reservoirs. This includes the protection of aquifers against leaks and infiltration of leachate from waste dumps or waste piles, natural brine from Sebkha, discharges from desalination plants, and discharges from seawater in coastal areas (Abd-Elhamid et al. 2018). In the case of seawater intrusion, a cutoff wall can be defined as underground semi-impervious or impervious structures constructed along the coast in a coastal aquifer to limit the seawater intrusion phenomenon and preserve freshwater resources.

Depending on the locality and availability of construction materials, several types of cutoff walls could be used. These include clay dike, brick wall, stone masonry dam, concrete dam, ferroconcrete dam, plastic-tarred-felt sheets, sheet pile of steel, corrugated iron or PVC, and injection screen of bentonite and grout (Nilsson 1988). Cutoff walls have been constructed in many places around the world, including Brazil, USA, and Mexico, and in the following, the most known subsurface dam projects are presented.

In 1973, Japan constructed the first subsurface dam in Kabashima at a cost of 32 million Yen in order to prevent seawater intrusion. As reported by Nishigaki et al. (2004), other

Responsible Editor: Marcus Schulz

✉ Ezzeddine Laabidi
laabidimhe@yahoo.fr

Rachida Bouhlila
bouhlila.rachida@enit.utm.tn

[1] Laboratory of Modeling in Hydraulics and Environment (LMHE), National Engineering School of Tunis (ENIT), University of Tunis El Manar (UTM), Bp 37, Le Belvédère, 1002 Tunis, Tunisia

subsurface dams were constructed such as Ayasatogawa, Tsunegami, Tsushima, Nakajima, Miyakojima (at Sunagawa, Fukuzato, and Minafuku), Kikaijima, and Okinawa Island (at Komesu, Keiza, Kumejima) mainly for agricultural use.

The Ananganadi underground dam is one of the first subsurface dams constructed in India. Located in Kerala (Raju 1983), its length is about 150m and a width of 1m and a total construction cost was about 7.500 USD. By 1997, India has constructed five other subsurface dams with a total storage capacity of 273,712 m^3.

In 1983, South Korea started the construction of the first subsurface dam entitled I-an. After that, in 1986, four other subsurface dams were constructed: U-il, Gocheon, Okseong, and Namsong. Their length ranges from 89 to 800m (Nishigaki et al. 2004).

In 1995, the collaboration between the Ministry of Agriculture of Burkina Faso and the Japan Ministry of the Environment started the construction of the first subsurface dam in Burkina Faso located at Nare Bridge. The underground dam is 8m high and 210m long and has a storage volume of 800,000m^3 (Nishigaki et al. 2004).

The physical barriers as a seawater intrusion control method have been developed in the last few decades by many researchers. The most recent studies are as follows.

Abdoulhalik et al. (2017) proposed a new method for seawater intrusion control, which is composed of a combination of an impermeable cutoff wall and a semi-permeable subsurface dam. Through the experiment laboratory and the simulation results using the code SEAWAT (Guo and Langevin 2002), the authors show that the mixed physical barrier proposed could produce better seawater intrusion reduction and a lower cost than the traditionally used barriers.

Armanuos et al. (2019) carried out experimental and numerical work to assess the effect of a flow barrier wall, a recharge well, and a combination of these to control seawater intrusion in a coastal aquifer. The authors tested the effect of the wall embedment ratio and the freshwater injection ratio on the reduction of seawater penetration length.

Chang et al. (2019) presented numerical and experimental investigation to test the performance of a subsurface dam on preventing seawater intrusion. The authors carried out a series of laboratory tests and numerical simulations to assess the effects of dam height, distance from the seaside boundary and head differences between the subsurface dam, and the fresh groundwater discharge.

Ebeling et al. (2019) conducted a series of simulations (a set of 542 remediation scenarios) in order to check the mixed hydraulic barrier approach as a solution for preventing seawater intrusion in a coastal aquifer. The authors demonstrate that hydraulic conductivity and regional freshwater flow are the most significant for the remediation time frame. The main finding is that the effectiveness of the presented solution is very sensitive to the rate and the location of the barriers.

Armanuos et al. (2020) examined the effect of using a barrier for controlling seawater intrusion in a sloped unconfined aquifer. The authors used the SEAWAT code to simulate the effectiveness of the barrier as a solution to prevent seawater intrusion. The authors show that the repulsion ratio is increased with increasing barrier depth. The outcomes of this study can be considered by decision-makers as a management solution for a coastal aquifer.

All the previous studies represent a contribution for verifying and testing the effectiveness of a physical cutoff wall as a solution to prevent saltwater intrusion. Several construction materials are used to set up the cutoff wall such as clay dike, brick wall, stone masonry dam, concrete dam, ferroconcrete dam, plastic-tarred-felt sheets, and sheet pile of steel. The important revealed conclusion is that control of saltwater intrusion using cutoff wall is a viable method but it could be costly in terms of construction techniques, operation, maintenance, and monitoring (Abd-Elhamid et al. 2018). This work presents a modeling study to assess the effectiveness of a new technique based on creating a seawater intrusion cutoff wall by calcite precipitation. This solution will very strongly reduce permeability and thus reduce a possible inflow of liquid. This new method is based on the development of a geochemical cutoff wall by the mixing in situ of Na_2CO_3 and $CaCl_2$ solutions. The purpose of this work is to analyze (1) geochemically the development of calcite cutoff wall by mixing two solutions; (2) as a relevant example of the use of this technique, the effect of the calcite cutoff wall on saltwater dynamics is tested; and (3) the effectiveness of the newly developed cutoff wall in protecting freshwater resources in a coastal aquifer is evaluated. Numerical simulations that assess the viability of this technique as a new technique to prevent seawater intrusion in a coastal aquifer are investigated. To the best of our knowledge, these objectives have never been investigated in previous studies. This work is carried out using the density-dependent flow and reactive transport code GEODENS (Bouhlila 1999; Bouhlila and Laabidi 2008; Laabidi and Bouhlila 2015; Laabidi and Bouhlila 2016).

Materials and method

Approach and investigated configurations

The simulations of the technique of construction of an underground cutoff wall by in situ precipitation of calcite are therefore carried out here on the problem of seawater intrusion into coastal aquifers and its reduction or even cancellation. The Henry problem has been widely used as a test case (benchmark) of density-dependent groundwater flow models. To provide general results, these processes are simulated using the Henry problem geometry with the same hydrodynamic parameters and boundary conditions (Henry 1964).

The Henry seawater intrusion problem concerns a vertical slice through an isotropic, homogeneous, confined aquifer. For the flow boundary, a freshwater constant flux is applied from the inland boundary and a hydrostatic pressure is distributed on the sea boundary. As shown in Fig. 1, L denotes the length of the aquifer and d its width. X_w is the distance between the cutoff wall and the seaside boundary and Zw is the cutoff wall depth. The aquifer parameters and the geometrical dimensions used in the simulated configuration are summarized in Table 1.

The cutoff wall is developed by a geochemical precipitation reaction of cement, caused by the injection of two solutions in two wells drilled parallel to the coastline, at a given distance from it; two solutions Na_2CO_3 and $CaCl_2$ are injected in parallel in the desired position (X_w) of the cutoff wall. The configurations simulated in this work are presented in Table 2.

The flux of the two injected solutions is maintained at $1\times10^{-6}m^3/s$ considerably less than the freshwater flux to answer the non-influence of the solutions flux on the dynamics of seawater.

Calcite will precipitate upon contact of $CaCl_2$ with Na_2CO_3 according to Eq. (1), and the precipitation will continue along the solution mixing zone (Laabidi and Bouhlila 2017; Saneiyan et al. 2018) until the total clogging of the pores in this section and the formation of a barrier to the flow across the constructed wall.

The reactive transport modeling highlighted the formation of a calcium carbonate mineral phase within the mixing zone between the two solutions, which controlled the spatial distribution of calcite in the injected zone.

$$Na_2CO_3(aq) + CaCl_2(aq) = CaCO_3(s) + 2NaCl(aq) \quad (1)$$

The concentrations of the master species of the two boundary solutions used in the simulations were calculated using the code PHREEQC (Parkhurst and Apello 1999) and are displayed in Table 3. Referring to Plummer (1975), if the mixing ratio in the mixing region is high and pCO_2 is low (normal atmospheric partial pressure), carbonate precipitation may occur. Accordingly, calculations were performed under the assumption of equilibrium with partial $CO_2(g)$ of $3.16\cdot10^{-4}$ bar, corresponding to the concentration of CO_2 in the atmosphere.

Precipitation of calcite occurs in the contact zone between the two injected solutions, in the area between the two injected wells. Precipitation induces a gradual decrease in media capacities for flow as the pores become filled by the precipitated calcite. The porosity decrease induces necessarily a reduction in permeability.

Table 1 Parameters used in Henry's problem

Parameter	Value	
L	2 m	Domain length
d	1 m	Domain thickness
ϕ	0.35	Porosity
k	1.00×10^{-9} m^2	Permeability
d_0	6.60×10^{-6} m^{2}s^{-1}	Molecular diffusion coefficient
q_b	6.60×10^{-5} ms^{-1}	Freshwater flux
ρ_0	1000 kgm^{-3}	Freshwater density
ρ_s	1025 kgm^{-3}	Seawater density
α_l	0.0 m	Longitudinal dispersivity
α_t	0.0 m	Transverse dispersivity
μ	0.001 kgm^{-1}s^{-1}	Fluid viscosity
g	9.81 ms^{-2}	Gravitational acceleration

Governing equations

The equations governing the movement of a fluid through saturated porous medium subject to variable-density conditions can be obtained from the mass and the momentum conservation principles. The following section presents briefly these governing equations (Bear 1988; Diersch and Kolditz 2002). For this study, only two-dimensional flow is considered. The fluid mass conservation equation is expressed as follows:

$$\frac{\partial}{\partial x_i}(\rho q_i) - \frac{\partial(\rho\phi)}{\partial t} + Q_m = 0 \quad (2)$$

where ϕ [L3L^{-3}] is the porosity, ρ [ML^{-3}] is the fluid density, Q_m [ML^{-3}T^{-1}] is the source/sink term (the mass flux per unit of volume), q_i is Darcy's velocity, and t [T] is the time.

GEODENS (Bouhlila 1999; Bouhlila and Laabidi 2008; Laabidi and Bouhlila 2015; Laabidi and Bouhlila 2016) describes two-dimensional transient convective, diffusive-dispersive, and reactive transfer of specie $\alpha(\alpha = 1, N_\alpha)$ using a sequential iteration approach of the following equation:

$$L(C^\alpha) + Q_m C^\alpha + \phi f^\alpha = \frac{\partial(\rho\phi C^\alpha)}{\partial t} \quad (3)$$

C^α [MM^{-}1] is the concentration of solute α, and N_α is the total number of species; Q_m is the source term and $L(C^\alpha)$ represents the transfer operator applied to C^α including the convection and the diffusion-dispersion phenomena and is expressed as follows:

$$L(C^\alpha) = \frac{\partial}{\partial x_i}\left\{\rho\phi D_{ij}\frac{\partial C^\alpha}{\partial x_j} - \rho\phi u_i C^\alpha\right\} \quad (4)$$

where i and j range from 1 to 2 for a two-dimensional flow and transport problem; u_i [LT^{-}1] is the effective velocity and is calculated by the following expression:

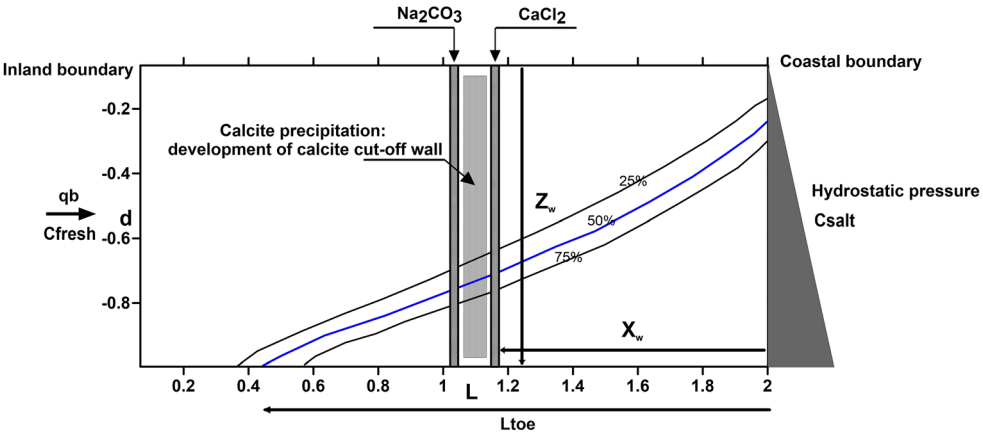

Fig. 1 Geometry and boundary conditions of the investigated configuration

$$q_i = u_i\phi = -\frac{K_{ij}}{\mu}\left(\frac{\partial p}{\partial x_j} - \rho g_j\right) \tag{5}$$

where q_i [LT⁻1] is Darcy's velocity, K_{ij} [L^2] is the intrinsic permeability, μ [$ML^{-1}T^{-1}$] is the fluid viscosity, p is the fluid pressure, g_j is the gravitational acceleration, and D_{ij} [L^2T^{-1}] is the diffusion-dispersion term and is expressed as follows:

$$D_{ij} = (d_0 + \alpha_T u)\delta_{ij} + (\alpha_L - \alpha_T)\frac{u_i u_j}{u} \tag{6}$$

where $\alpha_L[L]$ and $\alpha_T[L]$ are the longitudinal and the transversal dispersivity, respectively, d_0 [L^2T^{-1}] is the molecular diffusion coefficient, u_i [LT^{-1}] is the velocity vector component in the i direction, u_j [LT^{-1}] is the velocity vector component in the j direction, u [LT^{-1}] is the norm of the velocity vector, and δ_{ij} is the Kronecker delta function.

The f^{α} term represents the geochemical mass flux of species α. If N_r is the number of reactions related to the specie α, f^{α} is calculated as the sum of all the reactions which contribute to this mass flux (Bouhlila 1999; Bouhlila and Laabidi 2008; Laabidi and Bouhlila 2015; Laabidi and Bouhlila 2016), and is written as follows:

Table 2 Simulated locations and cutoff wall depth

Configuration	X_w	Z_w
C1	X_w=1.06-0.95-0.83-0.72-0.61-0.50	−1
C2		−0.9
C3		−0.8
C4		−0.7
C5		−0.6
C6		−0.5
C7		−0.4

$$f^{\alpha} = \sum_{r=1}^{N_r} \rho\left(\frac{\partial C^{\alpha}}{\partial t}\right)_r \tag{7}$$

The geochemical flux of each specie α at the time step Δt is calculated as the mass change of this specie during dissolution-precipitation reactions.

Impact on porosity and permeability

The physicochemical processes are written in GEODENS (Bouhlila 1999; Bouhlila and Laabidi 2008; Laabidi and Bouhlila 2015; Laabidi and Bouhlila 2016) at the macroscopic scale. The pore geometry is continuously modified by the dissolution-precipitation reactions of salts. The porosity at any finite element of the mesh and at every time step Δt is updated as follows:

$$\phi(t + \Delta t) = \phi(t) + \sum_{js=1}^{N_s} r_{js} V_{js} \Delta t \tag{8}$$

where V_{js} [L^3M^{-1}] is the molar volume of the salt j, r_{js} [$M^{-1}L^{-3}T^{-1}$] is the rate of the mineral precipitation (−) or dissolution (+), and N_s is the total number of salts.

For the modeling of the relation between porosity and permeability, capillary tubes or plane crack models have been used and can give relatively simple relationships between these two parameters such as the Koseny-Carman formula (De Marsily 1981). Sanford and Konikow (1989) proposed an empirical model for the sedimentary rocks to represent the permeability changes due to the dissolution or precipitation reaction of calcite in a coastal aquifer as follows:

$$Log(k) = a\phi - b \tag{9}$$

According to these authors, for sedimentary rocks, a is about 20 and b is deducted from the initial known values of k and ϕ.

Table 3 Concentration of master species of the two injected solutions

Master species (g/kg-water)	Na^+	H^+	$Ca2^+$	Cl^-	OH^-	HCO_3^-	CO_3^{2-}
Solution 1: $CaCl_2$	2.30E−9	3.07E−6	1.790	3.18	9.30E−8	1.56E−4	6.28E−9
Solution 2: Na_2CO_3	1.870	2.05E−10	5.08E−10	3.55E−9	1.34E−3	2.260	1.270

Kinetics of calcite precipitation

The undersaturation or the supersaturation of calcite in the mixture zone induces dissolution or precipitation of the carbonate rocks respectively. Many authors studied the kinetics of calcite dissolution-precipitation reaction in low-temperature aqueous systems. We can find in Sanford and Konikow (1989) and in Freedman and Ibaraki (2002) a detailed description of this process. In fact, evaporates dissolution-precipitation reactions are rather limited by ion diffusion processes into the aqueous solutions. Then, they can be written as first-order reactions. In GEODENS code (Bouhlila 1999; Bouhlila and Laabidi 2008; Laabidi and Bouhlila 2015; Laabidi and Bouhlila 2016), the kinetics of salts dissolution or precipitation reactions are represented by the geochemical flux, f^{α} (Eq. 7), and is written as follows:

$$\phi f^{\alpha} = \sum_{r=1}^{N_r} \rho \phi k_{cr} (1-\Omega_r) \tag{10}$$

where Ω_r is the saturation index of the salt r, and k_{cr} [$MT^{-}1$] is the kinetics coefficient of the reaction.

Results and discussion

Calcium carbonate precipitated along the mixing zone between the two solutions containing $CaCl_2$ and Na_2CO_3, which flowed in parallel during reactions. The formation of calcite started in a narrow zone where the two solutions are injected and this can be seen clearly in Fig. 2a. After 20 h of simulation time, the calcite formation spreads along the mixing zone until a total clogging of the injected area and the formation of the cutoff wall. Figure 2b and c show the porosity reduction and the hydraulic permeability decrease respectively after 5, 10, and 20h of injection time.

The initial condition was set as the steady-state saltwater wedge for the base case, the Henry problem without cutoff wall where the 10% contour intercept the aquifer bottom at x=1m from the shoreline. The parameter used to test the effectiveness of the geochemical cutoff wall as a technique to prevent seawater intrusion is the penetration of the seawater intrusion wedge. The penetration of the seawater intrusion wedge noted L_{toe}, as shown in Fig. 1, is calculated as the distance between the seaside boundary and the point where the 50% freshwater-seawater mixing isoline intersects the aquifer bottom.

To assess the effectiveness of the developed cutoff wall, a baseline case with no cutoff wall installed was first studied to be used as a benchmark for the investigated configurations. The effectiveness of the geochemical cutoff wall was characterized by the percentage of reduction of the penetration length $R = (L_{toe0} - L_{toe})/L_{toe0}$, where L_{toe0} and L_{toe} are the penetrations of the seawater intrusion wedge before and after the development of the cutoff wall, respectively.

The initial condition was set as the steady-state saltwater wedge for the base case where the 10% isoline intercepts the aquifer bottom at x=1m. The flux of the two solutions is maintained at $1\times10^{-6}m^3/s$, considerably less than the freshwater flux to answer the non-influence of the solutions flux on the dynamics of seawater. The cutoff wall depth and location are tested.

The parameter used to test the effectiveness of the geochemical cutoff wall as a technique to prevent seawater intrusion is the penetration of the seawater intrusion wedge. As shown in Fig. 1, the penetration of the seawater intrusion wedge noted L_{toe} is calculated as the distance between the seaside boundary and the point where the 50% mixing isoline intersects the aquifer bottom.

To assess the effectiveness of the developed cutoff wall, a baseline case with no cutoff wall installed was first studied to be used as a benchmark for the investigated configurations. The effectiveness of the geochemical cutoff wall was characterized by the percentage of seawater penetration reduction $R = (L_{toe0} - L_{toe})/L_{toe0}$, where L_{toe0} and L_{toe} are the penetration of the seawater intrusion wedge before and after the development of the cutoff wall, respectively.

Effect of cutoff location

As presented in Table 2, six positions from the seaside boundary were used to develop a geochemical cutoff wall (X_w=1.06m, 0.95m, 0.83m, 0.72m, 0.61m, and 0.50m) under the same flow and transport conditions. All the results are compared to the baseline case. Figure 3 describes the location of the development of a calcite cutoff wall in the desired locations after 20h of injection time. The precipitated quantity of calcite is about 8000 mol/m^3 generates a total clogging of the aquifer in the injection zone result of porosity decreasing. As shown in Fig. 3, we can notice that the saltwater wedge

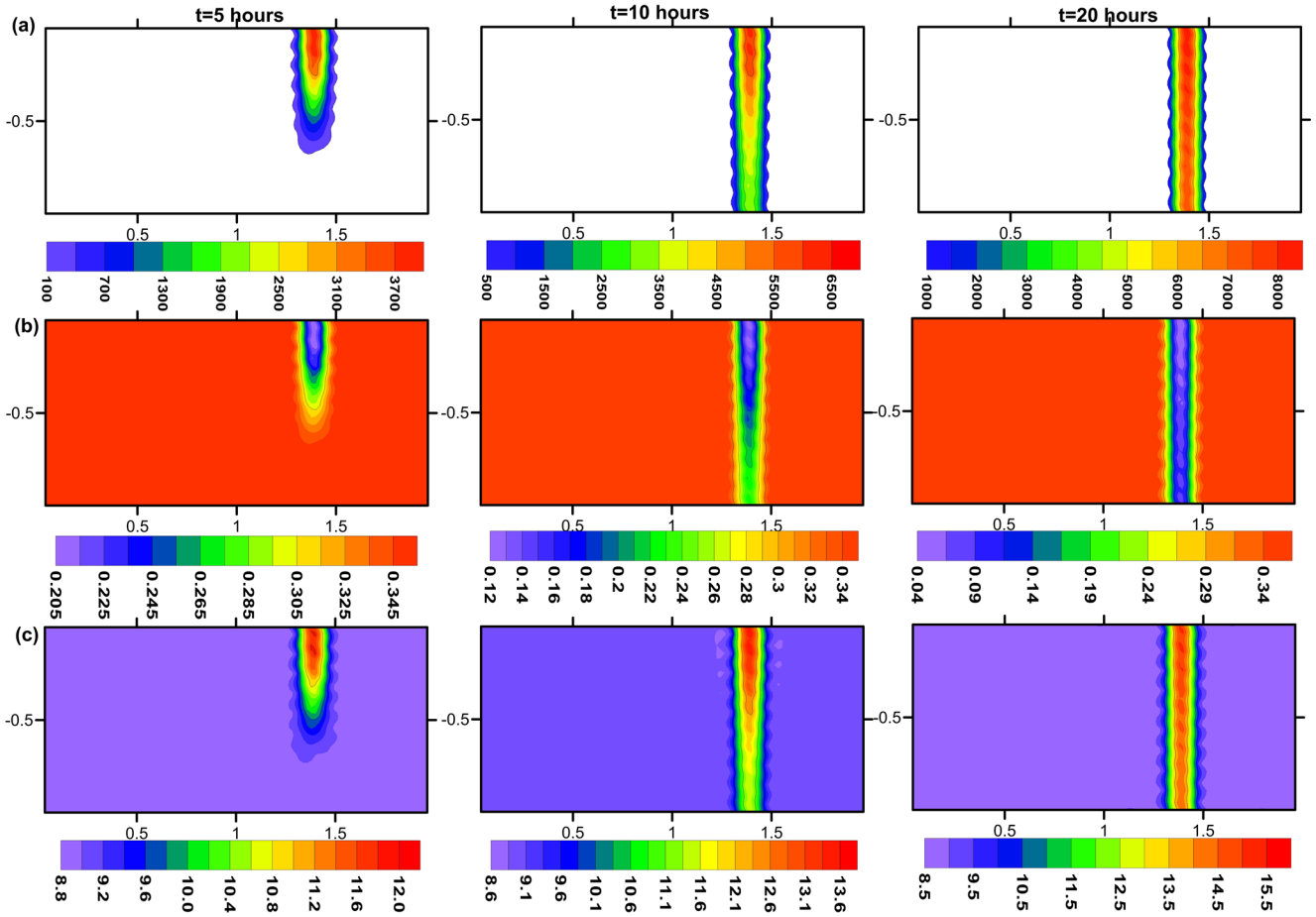

Fig. 2 Development of the geochemical cutoff wall after 5, 10, and 20 h of simulation time. **a** Calcite accumulation (mol/m^3); **b** porosity development; **c** permeability development: −Log (k) (m^2)

decreases to a minimum value and the penetration is stopped by the developed calcite cutoff wall after 20 h of injection time. Figure 4 illustrates the penetration decrease which reaches a minimum value fixed by the position of the two injection wells.

As presented in Fig. 4, the penetration length recorded in the base case is about 91.48 cm and the minimum penetration length was recorded in the position X_w=0.5 and is about 28.9, which corresponds to a percentage of reduction R of 68.41%. Maximum penetration length was recorded in X_w=1.06 and is about 73.04, which corresponds to a percentage of reduction R of 20.16%.

Effect of cutoff depth

The flux of the two solutions was kept at 1×10^{-6} m^3/s. All the locations (distance of the developed cutoff wall from the seaside boundary) described above are tested. The geochemical cutoff walls were developed at 1m, 0.9m, 0.8m, 0.7m, 0.6m, 0.5m, and 0.4m depths. Figure 5, Fig. 6, and Fig. 7 show the porosity decrease in the developed cutoff wall, velocity field, and Cl^- isoline contours at X_w=0.72m after 5, 10, and 20h of simulation time at a depth equal to 0.9 m, 0.7 m, and 0.5 m respectively.

After 5 h of simulation time, the quantity of precipitated calcite is considerably increased. As a result of calcite deposition, porosity is decreased from 0.2 after 5 h to about 0.035 after 20 h of simulation time. The total clogging due to porosity decrease has a direct effect on the flow and transport problem; the velocity field bypassed the clogging zone.

Figure 8 presents the penetration length in the position X_w=0.50 for different developed cutoff wall depths; minimum seawater penetration length was recorded at a depth equal to 0.9 m and is about 23.5 cm, which corresponds to a percentage of reduction R of 74.2%. Maximum penetration length at a depth equals to 0.4 m and is about 59.40 cm, which corresponds to a percentage of reduction R of 35.07 %.

Figure 9 presents the penetration length in the position X_w=0.83 for different developed cutoff wall depths. Minimum penetration length was recorded at a depth equal to 0.9 m and is about 49.3 cm, which corresponds to a percentage of reduction R of 46.07%. Maximum penetration length at a depth equals to 0.4 m and is about 73.34 cm, which corresponds to a percentage of reduction R of 19.84 %.

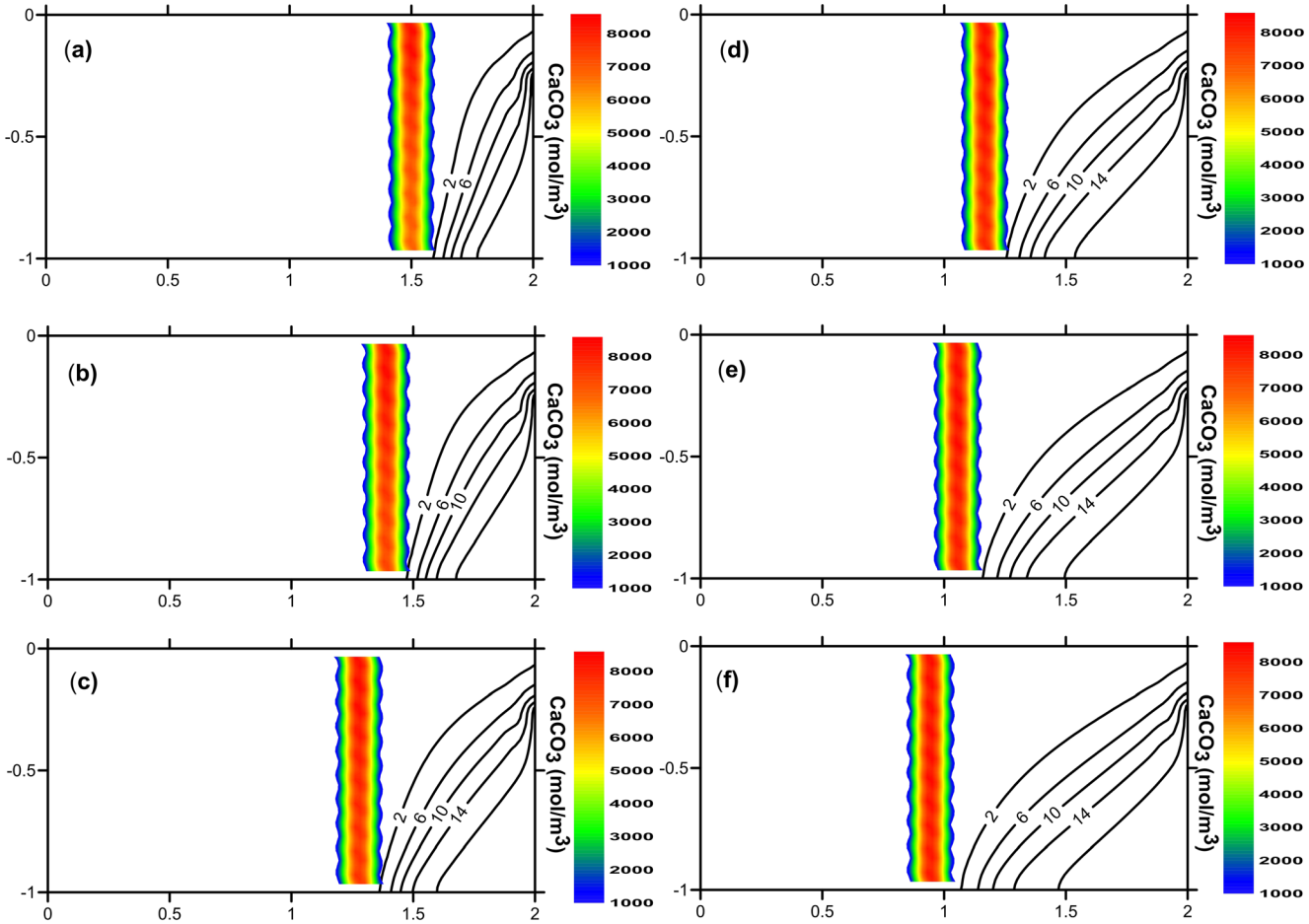

Fig. 3 Numerical simulations of the saltwater wedge after 20 h of simulation time with distance of the developed cutoff wall position from saltwater boundary of **a** 50 cm, **b** 61 cm, **c** 72 cm, **d** 83 cm, **e** 95 cm, and **f** 106 cm

As shown in Figs. 8 and 9, two stages of saltwater penetration are identified:

– Between 0 and 10 h: this stage is characterized by a significant decrease of seawater penetration length during the development of the geochemical cutoff wall. At the end of this stage, calcite deposit filled all the vertical section and porosity is significantly decreased and penetration length decreases and reaches minimum value.

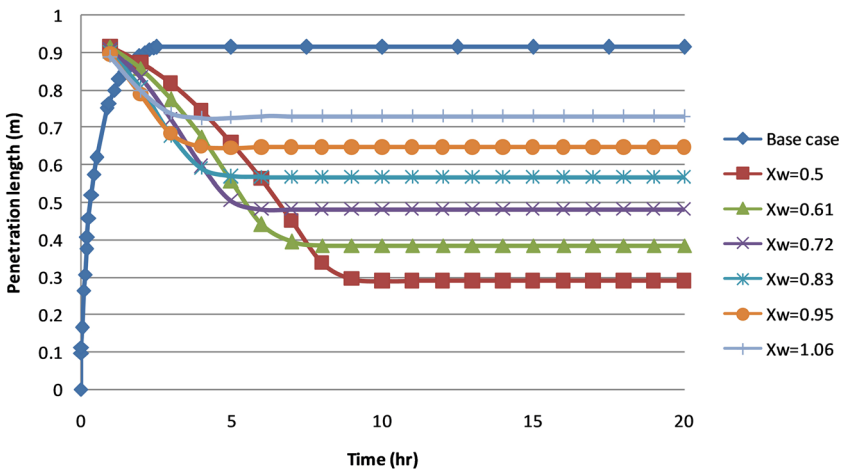

Fig. 4 Transient penetration of the seawater intrusion wedge for the base case and for a distance of the developed cutoff wall position from saltwater boundary of 50 cm, 61 cm, 72 cm, 83 cm, 95 cm, and 106 cm

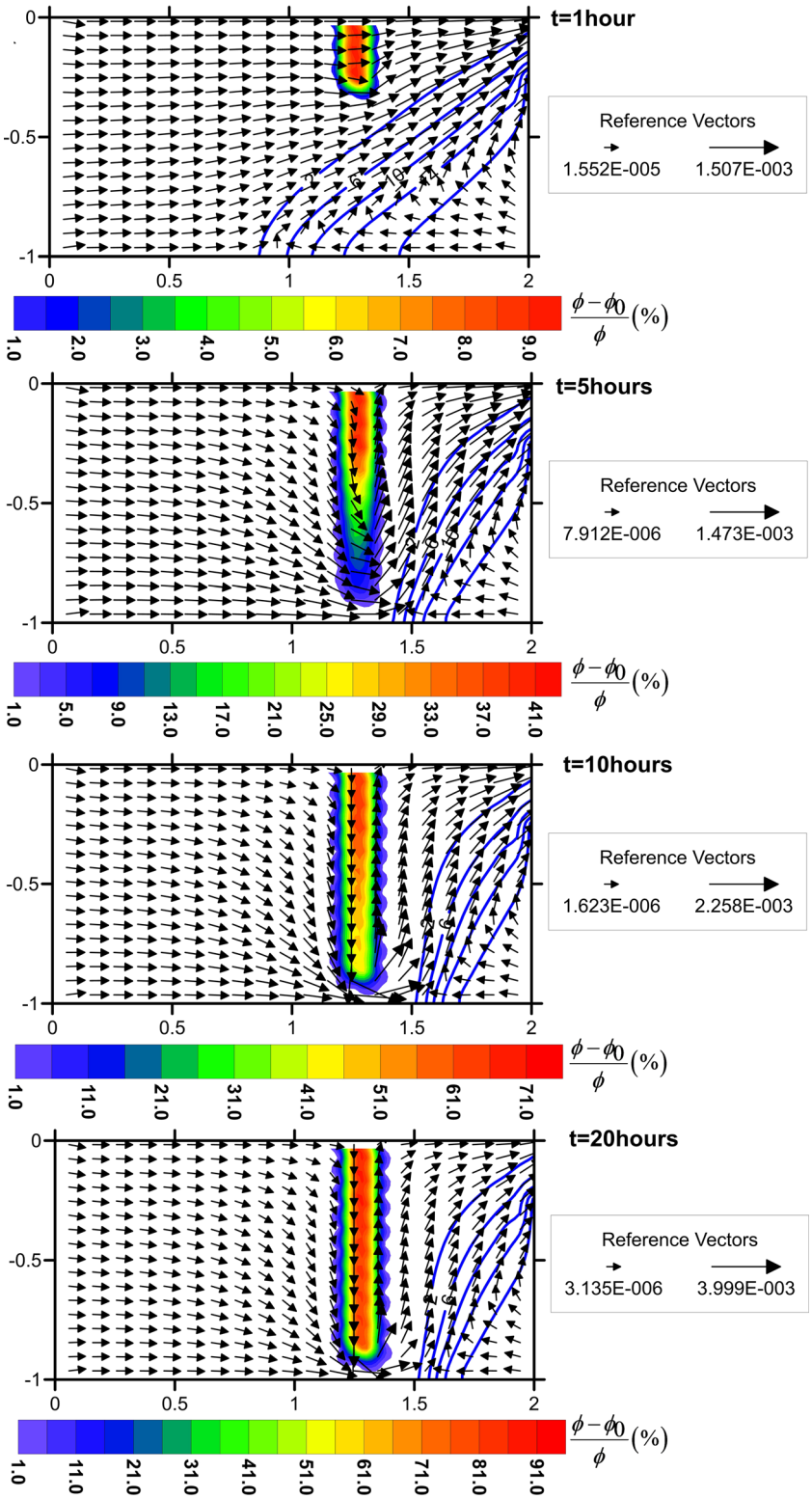

Fig. 5 Effect of the geochemical cutoff wall: % of porosity change, velocity field, and Cl^- isoline contours at X_w=0.72 and Z_w=0.9m

– Between 10 and 20 h: the saltwater penetration length becomes constant, the saltwater wedge reaches the dynamic equilibrium after 6 to 10 h depending on the depth of the cutoff wall.

Despite the expected result (normally, the more effective cutoff wall depth to prevent seawater intrusion is the whole aquifer thickness), the most effective depth preventing seawater intrusion is Z_w=0.9 m. At X_w=0.5, compared to the base

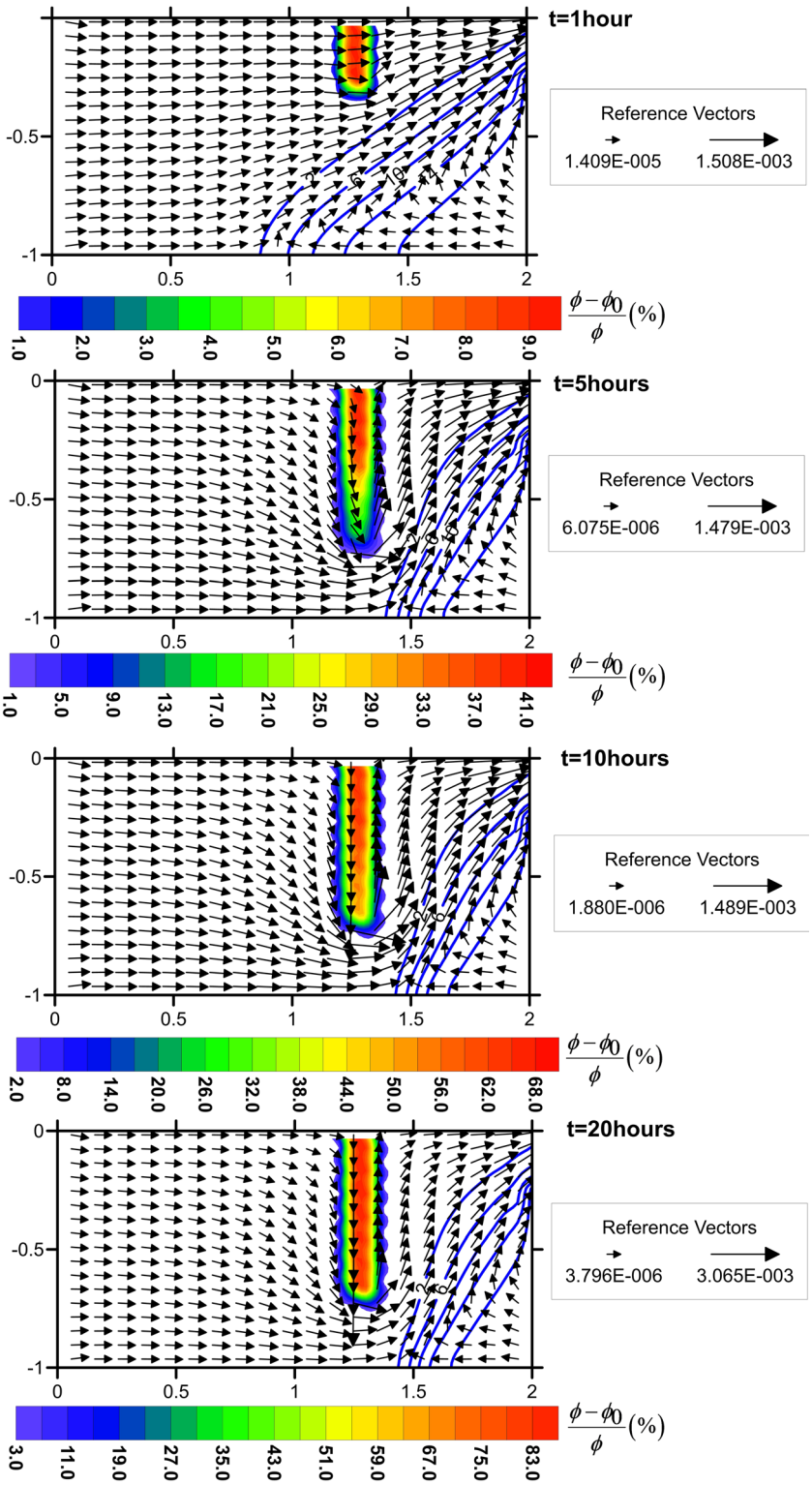

Fig. 6 Effect of the geochemical cutoff wall: % of porosity change, velocity field, and Cl^- isoline contours at X_w=0.72 and Z_w=0.7m

case, a reduction of 74.2% of seawater penetration length is created. As shown in Fig. 5, we can remark that after 5 h of simulation time, freshwater circuited the developed cutoff wall and flowed between the aquifer bottom and the bottom of the cutoff wall. The zone under the developed cutoff wall is characterized by a high magnitude of the velocity field, whereas the freshwater "pushes" the saltwater to the seaside boundary. After the trapping of the seawater contamination between the developed cutoff wall and the seaside boundary, the penetration saltwater wedge is significantly decreased.

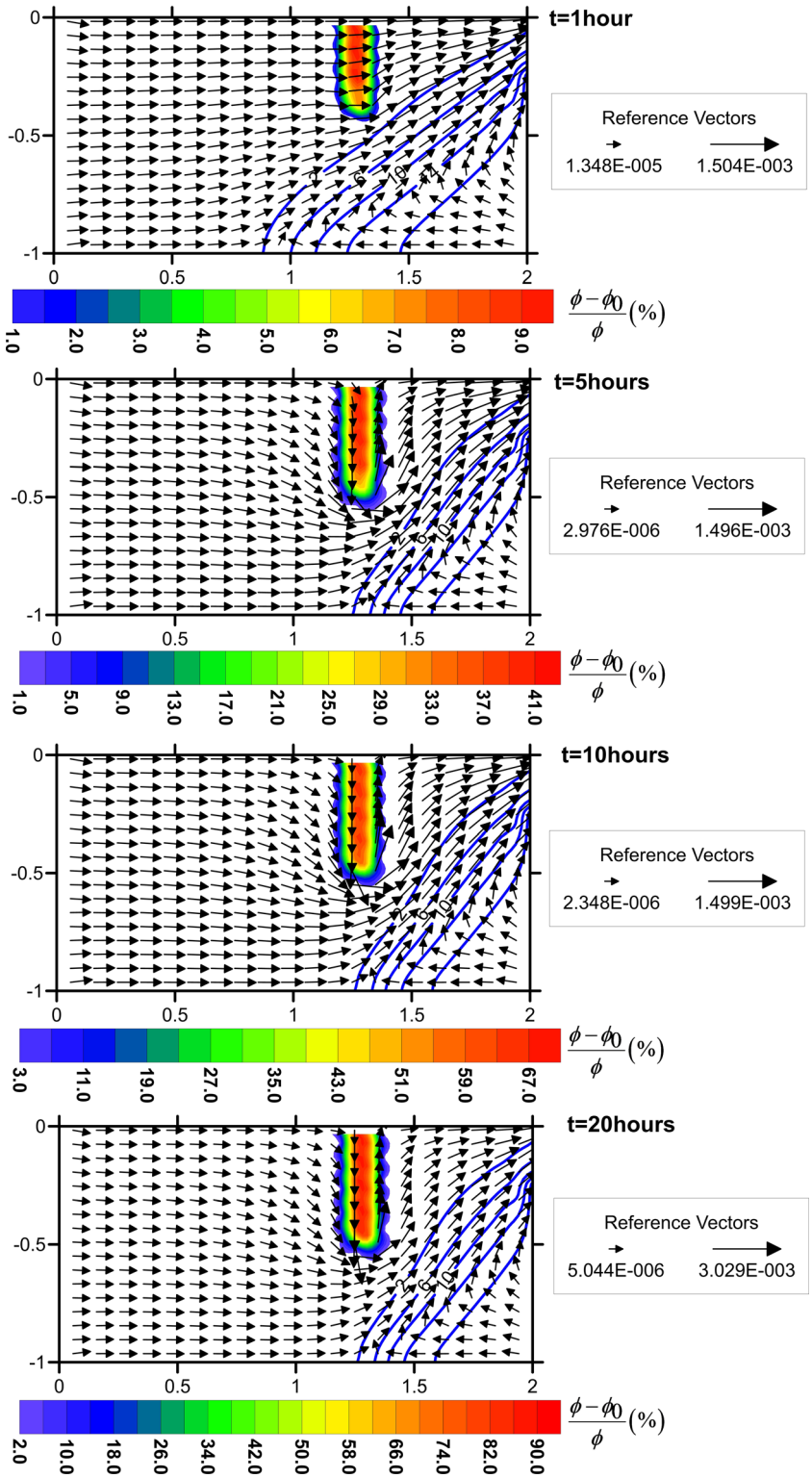

Fig. 7 Effect of the geochemical cutoff wall: % of porosity change, velocity field, and Cl^- isoline contours at X_w=0.72 and Z_w=0.5m

– At a depth equal to 1 m (the whole aquifer thickness), a reduction of 68.4% is calculated which corresponds to an increase of 5.8% of the saltwater penetration length compared to the result found at a depth equal to 0.9m.

– At a depth equal to 0.8 m, a reduction of 71.29% is calculated which corresponds to an increase of 2.91% of the saltwater penetration length compared to the result found at a depth equal to 0.9m. A reduction of 10% of cutoff

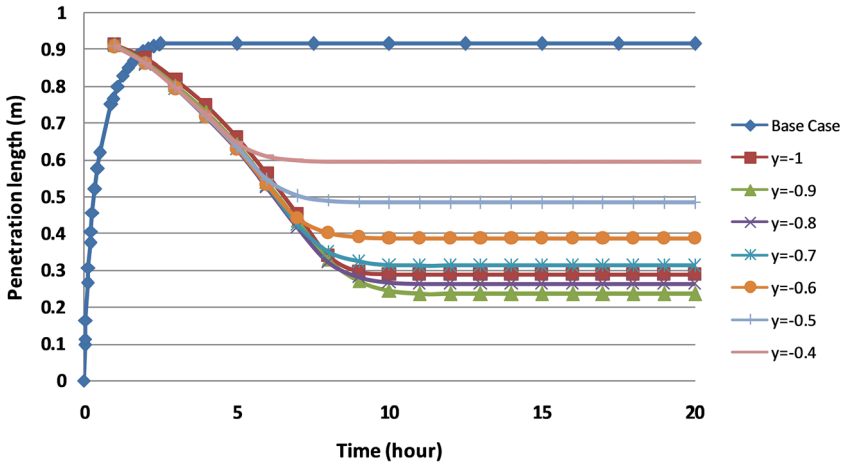

Fig. 8 Transient penetration of the seawater intrusion wedge for the base case at X_w=0.5 and for different depths of the developed cutoff wall of 1m, 0.9m, 0.8m, 0.7m, 0.6m, 0.5m, and 0.4m

wall depth gains only 2.91% of the seawater penetration length compared to the most effective case (which is a depth equal to 90% of the aquifer thickness).

– At a depth equal to 0.7 m, a reduction of 57.64% is calculated which corresponds to an increase of 16.5% of the saltwater penetration length compared to the result found at a depth equal to 0.9m.

Figure 10 shows the effect of the depth of the developed cutoff wall on the seawater penetration length for different cutoff wall positions. For all the simulated cutoff wall positions, the minimum seawater penetration length is at a depth equal to 0.9m. The seawater penetration length is minimum where the cutoff wall depth is ranging from 70 to 100% of the aquifer thickness. Due to the high cost of drilling, a cutoff wall depth equal to 70% of the aquifer thickness represents the optimum configuration to prevent seawater intrusion.

Conclusion

Groundwater contamination caused by seawater intrusion is a very common phenomenon in coastal aquifers. The increase of freshwater extraction from coastal aquifers due to touristic and agriculture activity has accelerated the degree of contamination of these freshwater resources. These activities can affect the quality and the volume of water in the coastal aquifer system.

A new method was suggested as a solution for preventing seawater intrusion. This new method is based on the development of a geochemical cutoff wall by the mixing of Na_2CO_3 and $CaCl_2$ solutions. The code GEODENS which is a density-dependent flow and transport model adequately predicts the geochemical problem and the behavior of saltwater dynamics after developing the cutoff wall. The paper makes the following major contributions:

- Calcite precipitates during mixing of Na_2CO_3 and $CaCl_2$ solutions under a normal atmospheric partial pressure of CO_2. Deposition of calcite starts around the inlet and continues along the mixing line which induces a total clogging where the porosity significantly decreases (porosity change reaches 95%).
- The developed cutoff wall is more effective in a depth ranging from 70 to 90% of the aquifer thickness. The presented results illustrate that there is a potential for

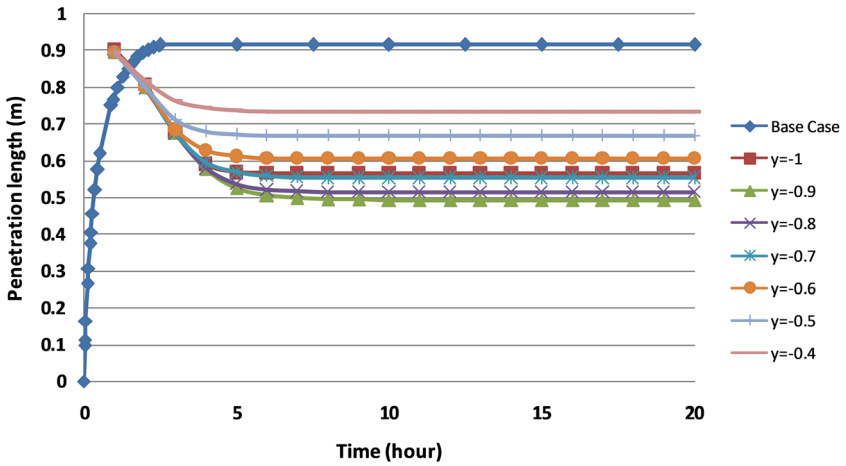

Fig. 9 Transient penetration of the seawater intrusion wedge for the base case at X_w=0.83 and for different depths of the developed cutoff wall of 1m, 0.9m, 0.8m, 0.7m, 0.6m, 0.5m, and 0.4m

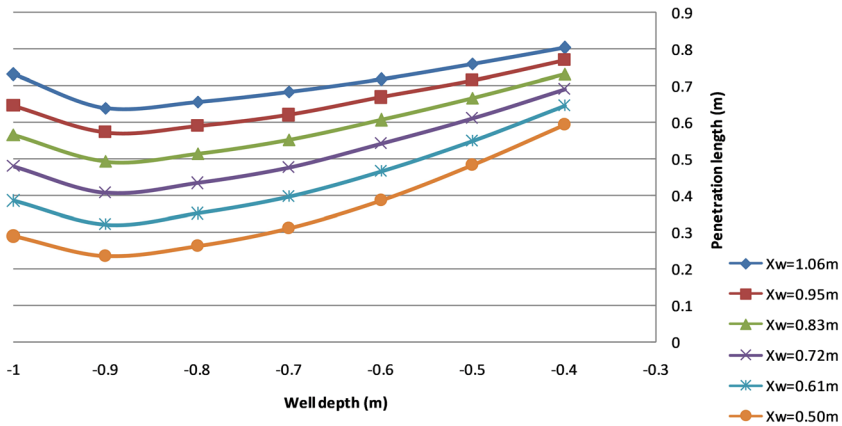

Fig. 10 Effect of the cutoff wall depth on the penetration of the seawater intrusion wedge for different cutoff wall positions

construction cost saving by developing a low-cost cutoff wall material for minimum depth.

- By the understanding of the main parameters that should be considered for high effectiveness of the developed cutoff wall, the results presented in this study will help in developing a new design of cutoff wall as a solution for preventing seawater intrusion. However, even if modeling results based on Henry saltwater intrusion problem showed satisfactory results regarding this new technique, attention has to be paid to the modeling of real cases regarding many reasons such as (1) effect of medium heterogeneity and complexity of geometry, (2) effect of real dispersivity and molecular coefficient values, (3) effect of radial flow around the injection wells which can be solved only by developing a three-dimensional model, and (4) development of a laboratory experiment (is ongoing) in order to validate the approach.

Author contributions Conceptualization and methodology: Ezzeddine Laabidi and Rachida Bouhlila. Simulations and results: Ezzeddine Laabidi. Manuscript preparation: Ezzeddine Laabidi. Review and editing: Rachida Bouhlila. Supervision: Rachida Bouhlila.

Data availability Most data generated or analyzed during this study are included in this manuscript. Further data used during the current study are available from the corresponding author on reasonable request.

Declarations

Ethics approval and consent to participate Not applicable.

Consent for publication Not applicable.

Competing interests The authors declare no competing interests. Patent was deposited in INNORPI Tunisia under number TN2020/0229.

References

Abd-Elhamid HF, Abd-Elaty I, Negm AM (2018) Control of saltwater intrusion in coastal aquifers. In: Groundwater in the Nile Delta. Springer, pp 355–384

Abdoulhalik A, Ahmed A, Hamill G (2017) A new physical barrier system for seawater intrusion control. J Hydrol 549:416–427

Armanuos AM, Al-Ansari N, Yaseen ZM (2020) Underground barrier wall evaluation for controlling saltwater intrusion in sloping unconfined coastal aquifers. Water 12:2403

Armanuos AM, Ibrahim MG, Mahmod WE, Takemura J, Yoshimura C (2019) Analysing the combined effect of barrier wall and freshwater injection countermeasures on controlling saltwater intrusion in unconfined coastal aquifer systems. Water Resour Manag 33:1265–1280

Bear J (1988) Dynamics of fluids in porous media. Courier Corporation

Bouhlila R (1999) Ecoulements, transports et réactions géochimiques couplés dans les milieux poreux. Cas Des Sels Et Des Saumures 280. https://doi.org/10.13140/2.1.2270.0808 (in French)

Bouhlila R, Laabidi E (2008) Impacts of calcite dissolution on seawater intrusion processes in coastal aquifers : density dependent flow and multi species reactive transport modelling. Anglais 320:220–225

Chang Q, Zheng T, Zheng X, Zhang B, Sun Q, Walther M (2019) Effect of subsurface dams on saltwater intrusion and fresh groundwater discharge. J Hydrol 576:508–519

De Marsily G (1981) Quantitative hydrogeology. Ed. Masson (in French)

Diersch H, Kolditz O (2002) Variable-density flow and transport in porous media: approaches and challenges. Adv Water Resour 25:899–944

Ebeling P, Händel F, Walther M (2019) Potential of mixed hydraulic barriers to remediate seawater intrusion. Sci Total Environ 693:133478

Freedman V, Ibaraki M (2002) Effects of chemical reactions on density-dependent fluid flow: on the numerical formulation and the development of instabilities. Adv Water Resour 25:439–453. https://doi.org/10.1016/S0309-1708(01)00056-2

Guo W, Langevin CD (2002) User's guide to SEAWAT; a computer program for simulation of three-dimensional variable-density ground-water flow.

Henry HR (1964) Effect of dispersion on salt encroachment in coastal aquifers. Hydrogeol J Water-Supply Pap 1613-C:70–84. https://doi.org/10.1007/s10040-004-0333-5

Laabidi E, Bouhlila R (2015) Nonstationary porosity evolution in mixing zone in coastal carbonate aquifer using an alternative modeling approach. Environ Sci Pollut Res 22:10070–10082

Laabidi E, Bouhlila R (2016) Reactive Henry problem: effect of calcite dissolution on seawater intrusion. Environ Earth Sci 75:655

Laabidi E, Bouhlila R (2017) Impact of mixing induced calcite precipitation on the flow and transport. Carbonates Evaporites 32:473–485

Nilsson A (1988) Groundwater dams for small-scale water supply. Intermediate Technology Publications

Nishigaki M, Kankam-Yeboah K, Komatsu M (2004) Underground dam technology in some parts of the world. J Groundw Hydrol 46:113–130

Parkhurst DL, Apello CAJ (1999) User's guide to PHREEQC – a computer program for speciation, Reaction-path, 1D-transport, and Inverse Geochemical Calculations. Technical Report 99-4259, US Geological Survey, USA. https://doi.org/10.1016/j.advwatres.2006.08.005

Plummer LN (1975) Mixing of sea water with calcium carbonate ground water geological society of America. Memoirs 142:219–236. https://doi.org/10.1130/MEM142-p219

Raju KCB (1983) Sub-surface dam and its advantages Proc Nat Sem Asses, Devt Magt GroundWater Res 29-30 April 1983, New Delhi:85-96

Saneiyan S, Ntarlagiannis D, Werkema DD Jr, Ustra A (2018) Geophysical methods for monitoring soil stabilization processes. J Appl Geophys 148:234–244

Sanford WE, Konikow LF (1989) Simulation of calcite dissolution and porosity changes in saltwater mixing zones in coastal aquifers. Water Resour Res 25:655–667. https://doi.org/10.1029/WR025i004p00655